Biomaterials

CrossMark

Hydrochar as protein support: preservation of biomolecule properties with non-covalent immobilization

Manuela Oliveira Castro[1] , Mayara Queiroz de Santiago[2] , Kyria Santiago Nascimento[2] ,
Benildo Sousa Cavada[2] , Emilio de Castro Miguel[3] , Amauri Jardim de Paula[4] ,
and Odair Pastor Ferreira[1,*]

[1] *Laboratório de Materiais Funcionais Avançados (LaMFA), Departamento de Física, Universidade Federal do Ceará,
P.O. Box 6030, Fortaleza, Ceará 60455-900, Brazil*

[2] *Laboratório de Moléculas Biologicamente Ativas (BioMol - Lab), Departamento de Bioquímica e Biologia Molecular, Universidade
Federal do Ceará, Fortaleza, Ceará, Brazil*

[3] *Central Analítica, Departamento de Física, Universidade Federal do Ceará, Fortaleza, Ceará, Brazil*

[4] *Solid-Biological Interface Group (SolBIN), Departamento de Física, Universidade Federal do Ceará, Fortaleza, Ceará, Brazil*

ABSTRACT

In this work, the ConBr lectin was non-covalently immobilized onto hydrochar (HC). This carbonaceous material was produced by the hydrothermal carbonization of glucose and then put to interact with the lectin, aiming to immobilize the biomolecule via electrostatic interactions. Samples obtained after the interaction were characterized by CHNS elemental analysis, scanning electron microscopy and Fourier transform infrared spectroscopy (FTIR). FTIR results from the conjugated sample identified the presence of NH_2^+ and NH_3^+ groups of the protein and COO^- groups of the HC, indicating the occurrence of electrostatic interaction between the biomolecule and the support. Furthermore, the immobilization experiment was also performed using ConBr lectin marked with fluorescein isothiocyanate to assess the immobilization on the hydrochar using fluorescence emission analysis. Hemagglutination tests revealed that even after the conjugation with the HC, the agglutinating property of lectin toward erythrocytes (red blood cells) was preserved. Finally, our results indicate that non-covalent interactions represent an efficient mechanism for protein immobilization on the HC while maintaining the protein structure and its biological activity.

Address correspondence to E-mail: opferreira@gmail.com

Introduction

Immobilization of biomolecules on materials and particles is a fundamental and highly used process in biomedicine and biotechnology, especially for the construction of biodevices and biocatalysts. For some biomolecules such as enzymes, it is a useful alternative to overcome issues like stability, manipulation and processing [1, 2]. On the other hand, for substrates, such as carbon nanotubes, the surface modification with a protein can improve its dispersion in water and promote reduction in its cytotoxicity [3, 4]. However, the preservation of the fundamental properties of both substrate and biomolecule during the immobilization/conjugation is still a challenge, considering that structural and stereochemical modifications of the biomolecule as well as the agglomeration of the substrate (if particulate) are possible.

In this sense, different immobilization approaches involving covalent and non-covalent interactions (hydrogen bonds, electrostatic and hydrophobic interactions, among others) can be used [2, 5]. Immobilization by covalent bonding has the advantage of reducing both instability and the possibility of components leaching from the generated system [2, 5]. However, this methodology usually requires modifications to the material surface, in order to generate functional groups which allow the formation of chemical bonds with the target molecule, and also experimental conditions that might affect structure and properties of the biomolecule and/or substrate [6]. In contrast, immobilization of active species through non-covalent interactions is a simple and cost-effective process comprising short-range stable interactions formed between the support (adsorbent) and the molecule of interest (adsorbate). Such interactions can occur themselves in a straightforward way in aqueous-based media with little impact on the biomolecule properties.

In biotechnological applications, a myriad of surface-immobilized biomolecules have been explored in the context of biocatalysis, biosensors and environmental remediation [6–11]. Among them, proteins catalyze and regulate numerous cellular processes and fundamental functions. Within this group, lectins are proteins of non-immune origin that can recognize and bind specific carbohydrate structures [12]. These proteins are found in animals and microorganisms, acting mainly in biological events of recognition, and in plants, mostly acting in defensive functions [13, 14]. ConBr is a D-glucose- and D-mannose-specific lectin isolated from *Canavalia brasiliensis* (Brazilian jackbean) seeds that present an agglutinating property toward erythrocytes (red blood cells). Additionally, ConBr presents various biological effects such as induction of paw edema in rats [15], in vitro stimulation of human lymphocytes [16], antidepressant effect in rats [17], neuroprotective effect [18] and antiproliferative effect in B16F10 cells [19].

In regard to substrates, carbon materials are attractive alternatives as biomolecule supports. The abundance of carbon in nature allows carbonaceous materials to be produced from different carbon sources and by different synthesis techniques, which result in materials possessing unique and tunable physical–chemical properties. Carbon nanotubes [20], graphene [21] and carbon quantum dots [22] are the most explored nanocarbons in studies of interaction with biomolecules and for biomedical and biotechnological applications. However, aspects regarding cost/yield and the morphological homogeneity of these nanocarbons must be considered. Differently, hydrothermal carbon (HC) has been little explored in biotechnology. It is obtained by hydrothermal carbonization, a simple, low cost, easy to scale up and environmental friendly method. In addition, there is the possibility of using biomass, biomass residues and carbohydrates as the carbon precursors [23–25].

Hydrothermal carbonization is performed in a closed reactor (autoclave) under mild temperatures (130–350 °C) with autogenic pressure, thus allowing the direct preparation of carbonaceous materials in a size range of a few micrometers and with a relatively high yield [26]. Reaction parameters and the carbon source used are factors that influence HC physical–chemical properties [25, 27, 28]. Hydrothermal carbon obtained from carbohydrates, for instance, exhibits characteristic morphology of dense spheres, which makes it attractive for environmental applications, such as adsorbents (for carbon dioxide, methane and hydrogen), catalysis and energy storage [25, 26]. In such applications, the spheres are usually activated via thermal treatments and functionalization. The as-prepared HCs have a high density of oxygenated functional groups on their surface (e.g., carboxylic acids, esters, ketones) [25, 26] and can be promising supports for biomolecule immobilization, since such surface chemical groups can act as anchoring and/or interaction sites for biomolecules.

In this work, ConBr lectin was used as a model biomolecule for accessing the support properties of hydrothermal carbon through non-covalent interactions. The substrate was prepared by hydrothermal carbonization of glucose and used without further modifications. After the interaction between lectin and the HC, the effectiveness of the method was tested regarding the immobilization of the biomolecule and, also, the maintenance of its biological function by exploring the hemagglutination activity of immobilized lectin.

Materials and methods

Materials

Materials were purchased from Sigma Aldrich, LGC Biotecnologia and Dinâmica and were used as received, without further treatment. All solutions were prepared using ultrapure water.

Preparation of hydrothermal carbon (HC)

HC was prepared by hydrothermal carbonization of 4.0 g of glucose [D(+)glucose anhydrous] dissolved in 35.0 mL of water. The resulting homogeneous solution was transferred to a Teflon cup (60 mL of capacity), which was inserted in a stainless steel autoclave. The reactor was submitted to heating at 180 ± 5 °C in muffle furnace for 24 h. After this period, the reactor was cooled in an ice bath. The solid portion (HC) was separated by vacuum filtration using polyvinylidene fluoride (PVDF) membrane of pore size 0.22 μm. In the following, HC was washed thoroughly with ultrapure water and dried at 70 °C.

Preparation of ConBr lectin

Canavalia brasiliensis seeds were collected in the state of Ceará, Brazil, peeled and ground in a mill until a fine powder was obtained. The soluble proteins were extracted by suspension in NaCl 0.15 mol/L, $CaCl_2$ and $MnCl_2$ 0.005 mmol/L solution [1:10 (m:v)], under constant agitation for 4 h at room temperature. The extract was centrifuged at $10000 \times g$ for 20 min at 4 °C, and supernatant (total extract) was put into Sephadex® G-50 affinity column (1.3 × 19 cm), previously equilibrated with NaCl 0.15 mol/L, $CaCl_2$

and $MnCl_2$ 0.005 mmol/L. Unbound material was eluted with the same solution, and lectin was eluted with D-glucose solution 0.1 mol/L [29]. The eluates collected in fractions of 3.6 mL were monitored by spectrophotometry at 280 nm and used for the determination of hemagglutination activity [30] and total protein content according to the protocol described by Bradford [31]. The fractions were dialyzed and lyophilized, and the homogeneity of the lectin was monitored using SDS-PAGE. The pure protein was used in posterior tests.

Preparation of ConBr lectin with fluorescein isothiocyanate (FITC)

ConBr was dissolved in a sodium bicarbonate buffer (0.1 mol/L, pH 9.0) at concentration of 5.0 mg/mL and incubated with its specific sugar methyl-α-D-mannopyranoside (0.1 mol/L) to block the carbohydrate recognition domain (CRD). After that, 62.5 μL of FITC was added to the solution containing the lectin with CRD blocked (1.0 mg/mL). Shielded from light, the lectin–sugar–FITC solution was submitted to mild agitation for 2 h. Lectin–sugar–FITC and unconjugated FITC were separated by molecular exclusion chromatography in a PD-100™ column. The material was eluted with sodium phosphate buffer 0.01 mol/L pH 7.4, containing KCl 0.027 mol/L and NaCl 0.138 mol/L. Aliquots of 1 mL were collected and analyzed in spectrophotometer at 280 and 495 nm. Collected fractions (absorbance values higher than 0.400) were submitted to dialysis against ultrapure water and then lyophilized.

Immobilization of ConBr lectin on HC

In order to promote lectin immobilization, HC and ConBr lectin were dispersed separately at 1 mg/mL in a 2-(N-morpholino)ethanesulfonic acid (MES) buffer 0.1 mol/L (pH 5.5). HC was dispersed using an ultrasound bath, and lectin was dissolved using a shaker. An HC dispersion (10 mL) was added to a lectin solution (16 mL) under agitation, and the system was kept under agitation for 17 h. After said time period, the sample generated was centrifuged at $1000 \times g$ in 5 min stages at room temperature and washed six times (10 mL each) using an MES buffer 0.05 mol/L (pH 6.5) and isolated by centrifugation at $1000 \times g$ in 10 min stages. The (HC–ConBr) sample generated was dried under vacuum at room

temperature until constant weight. The pH of an MES buffer was adjusted using NaOH 3 mol/L. The same procedures were also used to immobilize ConBr marked with FITC.

Evaluation of hemagglutination activity of ConBr lectin immobilized on HC

Hemagglutination activity was investigated by promoting contact between HC–ConBr and rabbit erythrocytes (an adult animal kept in a bioterium) treated with trypsin and using the methodology described by Ainouz et al. [32]. For the assays, samples were dispersed in a Tris–HCl buffer 0.05 mol/L (pH 7.6) containing NaCl 0.15 mol/L and then put in contact with treated erythrocytes for 30 min in an incubator at 37 °C and 30 min on the bench at room temperature. Assays were also performed using pure ConBr (positive control), pure HC and MES buffer (negative controls). To evaluate if the CRD of the lectin is responsible for the hemagglutinating activity, a hemagglutination inhibition assay was performed after incubating HC–ConBr with its specific carbohydrate, methyl-α-D-mannopyranoside, at 0.1 mol/L at 37 °C for 30 min.

Characterization

Morphology of the samples was investigated using scanning electron microscopy (SEM, Quanta450 FEG microscope, from FEI, 10–20 kV) and transmission electron microscopy (TEM, Tecnai20 microscope, from FEI). For SEM images, the samples (HC and HC–ConBr) were pulverized on carbon tape attached to Al stub or dropping an aqueous suspension of HC on Al stub and letting the water evaporate at room temperature. For TEM images, the samples were prepared by dropping an aqueous suspension of HC on a formvar-coated copper grid and also letting the water evaporate at room temperature. Quantification of carbon, hydrogen, nitrogen and sulfur contents in samples was obtained using CHNS elemental analysis (elemental analyzer from Fisons, model EA 1108 CHNS-O). The results were used for determining oxygen content in samples using the expression [$100\% - (wt\%C + wt\%H + wt\%N + wt\%S)$]. Chemical structure of the samples was analyzed using Fourier transform infrared spectroscopy (FTIR, Vertex 70v spectrometer, from Bruker). Vibrational

spectra were obtained using attenuated total reflection (ATR), with the platinum ATR accessory (Bruker) which contains a single reflection diamond crystal. Spectra were obtained under vacuum, in the mid-infrared region (4000–400 cm^{-1}) with 2 cm^{-1} resolution. Bands in the region between 1800 and 1480 cm^{-1} of the HC, ConBr and HC–ConBr spectra were analyzed by deconvolution, using Fityk open-source software version 0.9.8. Deconvolution was performed without baseline correction and using a Gaussian function. The hydrodynamic diameter and zeta potential (ζ) were obtained using dynamic light scattering (DLS) and electrophoretic light scattering (ELS), respectively (Zetasizer Nano ZS, from Malvern, He–Ne laser with 633 nm wavelength). Fluorescence emission of samples was evaluated using confocal scanning laser microscopy (LSM 710 microscope, from Zeiss, argon excitation laser of 488 nm). The emission was captured from 493 to 610 nm. Light microscopy images used to evaluate the erythrocyte agglutination were obtained using Eclipse 80i microscope from Nikon.

Results and discussion

To evaluate HC as a support for biomolecules, its morphological, compositional, structural and surface properties were characterized. Morphological aspects were analyzed by SEM and TEM images, as shown in Fig. 1a, b, respectively. The images show that hydrothermal carbon obtained by carbonization of glucose is formed by dense spherical-like particles, either isolated or coalesced in aggregates. Average particle diameter measured using micrographs was around 950 nm (Fig. S1). Additionally, the average hydrodynamic diameter of the particles was evaluated by DLS and it was also around 950 nm (Fig. S2), thus converging with that obtained by SEM. However, as shown in DLS analysis and SEM images, particles from approximately 200 nm–4 μm can be observed in HC sample.

The HC composition was determined by CHNS elemental analysis. The hydrochar is composed of carbon (65.01%), hydrogen (4.51%) and oxygen (30.48%) (Table 1). ELS analysis has shown that zeta potential (ζ) of HC is negative (−49.5 mV), indicating partial deprotonation of superficial oxygenated groups such as carboxylic acids when the
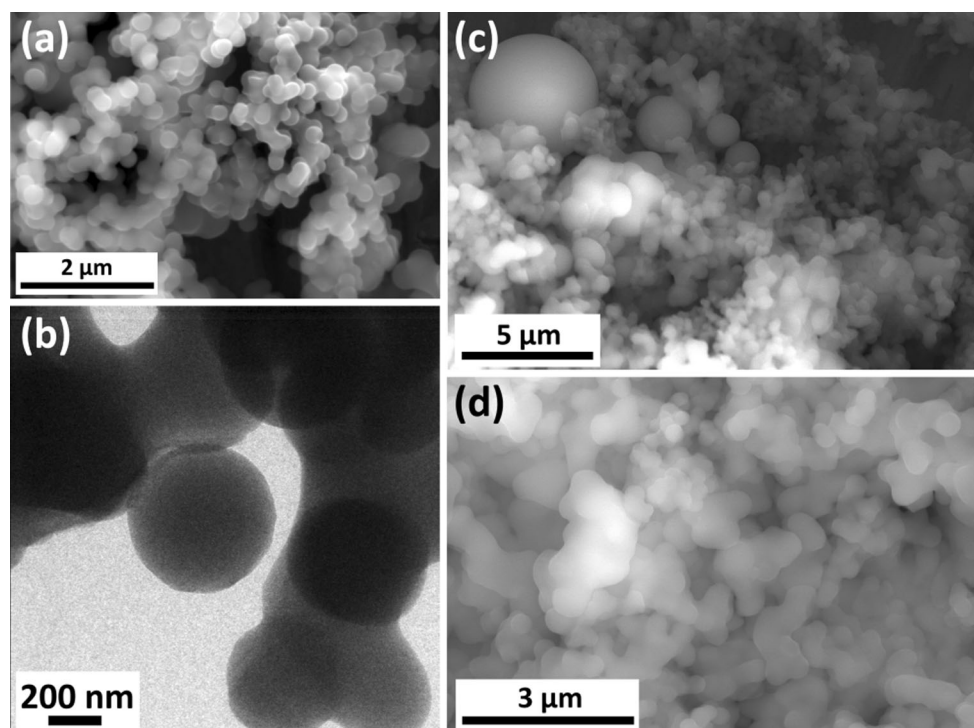
Figure 1 Morphological characterization. **a** SEM and **b** TEM images of the HC sample and SEM (**c**, **d**) images of the HC–ConBr sample.

Table 1 Carbon, hydrogen, nitrogen, sulfur and oxygen contents obtained by CHNS elemental analysis and also average hydrodynamic diameter and zeta potential measured by DLS and ELS, respectively

Samples	C (wt%)	H (wt%)	O[b] (wt%)	N (wt%)	S (wt%)	Molar ratio (N/S)	Average hydrodynamic diameter (nm)	Zeta potential (mV)
HC	65.01	4.51	30.48	0	0	–	950.6	−49.5
ConBr[a]	53.55	6.96	22.53	16.71	0.25	152.95	–	+6.53
MES[a]	36.91	6.71	32.78	7.17	16.42	1.00	–	–
HC–ConBr	59.64	4.98	30.03	3.95	1.40	6.41	–	–

[a] Carbon, hydrogen, nitrogen and sulfur contents for ConBr and MES calculated using following expression: wt% of element = [mass of the element in the molecule/molar mass of molecule] × 100%

[b]Oxygen contents for all the samples were calculated using the following expression: wt%O = [100% − (wt%C + wt%H + wt%N + wt%S)]

carbonaceous material is in the MES buffer 0.1 mol/L (pH 5.5) at 1.0 mg/mL (Table 1).

In the FTIR spectrum for HC (Fig. 2a), intense and broad bands are seen with maxima at 3396, 1701 and 1298 cm^{-1}. Such bands are characteristic of O–H, C=O and C–O stretching modes in carboxylic acid, respectively [24, 27, 33–36]. There are also bands at 1609 and 1509 cm^{-1}, corresponding mainly to C=C vibrations in aromatic moieties [24, 27, 33–36]. Since carbonyl is a functional group that has vibration modes which are very sensitive to surface chemical

modifications, a more detailed assessment was performed by deconvolution of the bands in the region between 1800 and 1480 cm^{-1} [37].

Deconvolution of the bands in the focused region of the HC spectrum (Fig. 2c) reveals modes at 1747, 1709 and 1679 cm^{-1}. The first component is typical of the carbonyl vibrations in ester, lactone, ketone and quinone, and the second and third are typical of carboxylic acid [27, 33–37]. Esters and ketones in the structure of HC from glucose were also found in others studies using X-ray photoelectron spectroscopy (XPS) [24] and
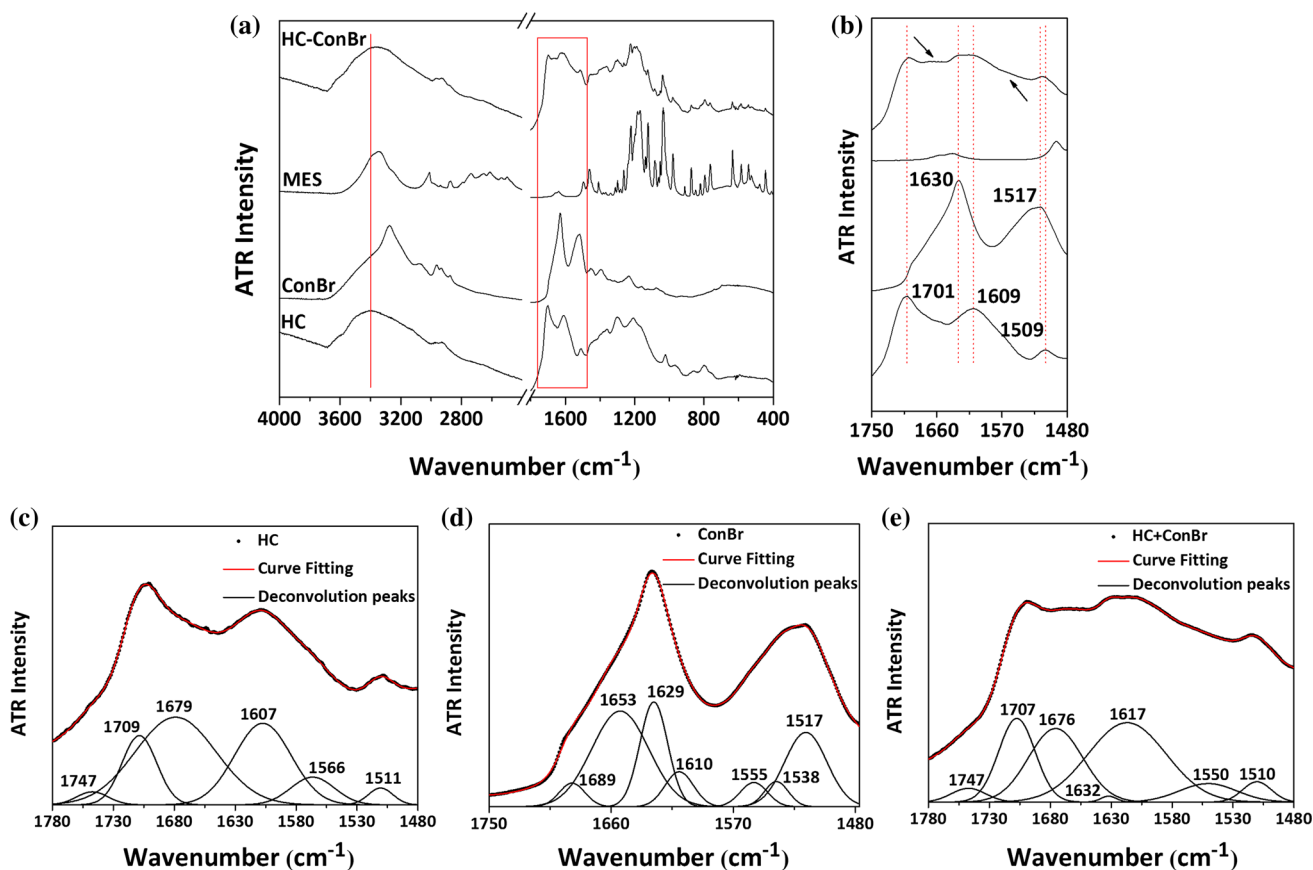
Figure 2 Structural characterization by FTIR. **a** Spectra of HC, ConBr, MES and HC–ConBr. **b** The same region shown by the *red outline* in image **a** is magnified. Deconvolution of the bands in the region between 1800 and 1480 cm^{-1} of FTIR spectra corresponding to **c** HC; **d** ConBr; and **e** HC–ConBr.

nuclear magnetic resonance spectroscopy (NMR) [28], respectively. The modes at 1607 and 1511 cm^{-1} are attributed to C=C stretches, and the component at 1566 cm^{-1} can be assigned to carboxylate ions.

Structurally, lectin is composed of identical subunits containing 237 amino acids with approximately 25 kDa each [14, 29, 38, 39]. The lectin can acquire dimeric or tetrameric conformations according to pH, being the equilibrium dislocated to tetrameric form (Fig. S3) in the pH 5.5 in which adsorption experiments were performed [38, 40, 41]. In the tetrameric form, ConBr has a diameter of about 4 nm [39]. Finally, it must also be considered that the equilibrium might be altered by the presence of the hydrochar, since this latter can lead to changes in pH mainly due to the presence of carboxylic acids on the HC surface. However, with the use of the MES buffer, this effect was prevented. ELS analysis of lectin solubilized in MES buffer 0.1 mol/L (pH = 5.5) at 1.0 mg/mL showed an average zeta potential value of +6.53 mV (Table 1). This value is explained by the

fact that the lectin possesses a theoretical isoelectric point at pH 5.84 [39]. In order to compare the structures of the hydrothermal carbon and the lectin, the CHNS elemental composition of the latter was calculated, using its chemical formula ($C_{1140}H_{1765}N_{305}O_{360}S_2$) as a starting parameter. These results are described in Table 1, along with the N/S molar ratio.

In the FTIR spectrum of ConBr (Fig. 2a) intense bands can be seen with maxima at 3329, 1630 and 1517 cm^{-1}, which are characteristic of N–H, C=O stretching modes and N–H deformations in amides, respectively [35, 42, 43]. For proteins, it is known that the band located in the region between 1700 and 1600 cm^{-1} has 80% of its intensity attributed to carbonyl stretching while the other 20% can be assigned to C–N, C–C–N and N–H vibrations [42, 43]. In addition, this band is very sensitive to the secondary structure of these biomolecules and results from those vibrations which originated from amino acid main chains (peptide bond) and also from side chains.

Deconvolution of the bands in the region between 1800 and 1480 cm^{-1} (Fig. 2d) makes it possible to find modes centered at 1689 and 1610 cm^{-1}, which can contain contribution of symmetric and asymmetric stretching modes of $CN_3H_5^+$ in arginine [42]. It is also possible to identify the components at 1629 and 1538 cm^{-1}. The first one can contain contributions of symmetric stretching of N–H in the NH_3^+ of lysine and of C=O stretching in amides [42]. The second can also have contribution of asymmetric stretching of N–H in the NH_3^+ of lysine. In the ConBr structure, lysine and arginine are side chain amino acids (Fig. S3) and, by being positively charged, could potentially be available for interaction with carboxylates present on the surface of the HC via electrostatic interaction.

The FTIR spectrum of the MES ($C_6H_{13}NO_4S$) buffer was also investigated, since the adsorption experiments used for interacting protein and HC and, also, the washing process of the final sample (HC–ConBr) were performed using this buffer. In Table 1, the calculated CHNS elemental composition and N/S molar ratio for MES are described. Additionally, Fig. 2a presents FTIR spectrum of the solid buffer, in which it can be observed two low intensity bands at 1656 and 1638 cm^{-1}. Due to this spectral profile for MES, there is little influence from the buffer in the region between 1800 and 1600 cm^{-1} analyzed for the HC protein sample even if it is still present in the final product (after washing). Thus, the focused spectral region may be used to access the lectin–hydrothermal carbon interactions and also to investigate changes in bands of the support and the protein due to interactions.

The HC–ConBr conjugate was also assessed on its morphological, compositional and structural aspects and on the properties of the immobilized protein. SEM images (Fig. 1c, d) show that the morphology of the particles and aggregates was not changed by the interaction with the lectin. On the other hand, CHNS elemental analysis of HC–ConBr suggests the immobilization of the lectin on the surface of the hydrothermal carbon, since the analysis revealed the presence of nitrogen (3.95%) and sulfur (1.40%), elements that are absent in the composition of the HC. The conjugate also has in its composition C (59.64%), H (4.98%) and O (30.03%) (Table 1). Although nitrogen and sulfur could be present in the sample after drying due to crystallization of MES buffer presents in the interparticle pores, analysis of the N/S molar

ratio in HC–ConBr (Table 1) also suggests that the lectin is supported on the hydrothermal carbon. The N/S molar ratio (6.41) of the sample is inferior to that of the isolated lectin, but superior to that obtained for MES. Therefore, nitrogen and sulfur present in the sample are not from the buffer alone, but also from the immobilized lectin. It is also worth mentioning that the MES buffer would not affect the protein–hydrochar interaction as shown by other studies involving the interactions occurring at the bio–nano interface of several nanoparticles and nanostructures [44, 45]. In other words, with the information in the current literature, we can assume that it is very unlikely that MES adsorb on the hydrochar surface to an extent that can prevent further lectin adsorption.

The FTIR spectrum of HC–ConBr shows some differences if compared with spectra of the HC and ConBr (Fig. 2a). For example, a shift in the maximum intensity of the large band between 3690 and 3000 cm^{-1} can be observed, if compared with the same region in the HC spectrum (from 3405 to 3366 cm^{-1}). This shift indicates that, in the HC–ConBr spectrum, there is an overlap of the bands corresponding to O–H vibrations in ConBr, HC and MES and N–H in ConBr. The contribution of MES to the HC–ConBr spectrum and its presence in the sample is supported by analysis of the bands in lower wavenumbers (between 1400 and 400 cm^{-1}). In this region, the typical bands of crystalized MES can be seen. In the region between 1800 and 1480 cm^{-1} (Fig. 2b), spectral alterations are evident through expansion of the region highlighted by the red rectangle in Fig. 2a. From the vertical dashed red lines, it can be seen that the spectrum of the sample HC–ConBr is a combination of the spectra corresponding to HC and to ConBr (Fig. 2b). First, a band corresponding to that of carbonyl in carboxylic acids in the HC spectrum can be identified. The difference in line profile and a small shift toward smaller wavenumbers between the maximum of the two bands suggests that the interaction with the lectin occurred between these functional groups. The spectral region between 1645 and 1580 cm^{-1} also possesses bands centered at 1630 cm^{-1} attributed to ConBr and at 1609 cm^{-1} assigned to HC. The band with a maximum at 1516 cm^{-1} seems to correspond to the band at 1509 cm^{-1} in the HC spectrum with some contribution of the band at 1517 cm^{-1} in the ConBr spectrum.

The arrows in Fig. 2b point to differences in line profile related to the same regions in the HC spectrum. Looking in detail at the deconvolution of the

bands between 1800 and 1480 cm^{-1} in the HC–ConBr spectrum (Fig. 2e), the spectral line elevation is caused by the overlap of the bands present in the HC and ConBr spectra. The elevation indicated by the downward arrow might result from the combination of the components centered at 1676, 1632 and 1617 cm^{-1}, while that indicated by the upward arrow would be resulting from the component at 1550 cm^{-1}. The component at 1676 cm^{-1} corresponds to that at 1679 cm^{-1}, estimated by deconvolution of HC (Fig. 2c). The component at 1632 cm^{-1} in the HC–ConBr spectrum corresponds to that centered at 1629 cm^{-1} in the deconvolution of ConBr (Fig. 2d). The width of the component at 1617 cm^{-1} suggests that it results from the sum of the components centered at 1607 cm^{-1} in the deconvolution of HC (Fig. 2c), and those centered at 1610 cm^{-1} in the deconvolution of ConBr (Fig. 2d). The large component at 1550 cm^{-1} is possibly formed by the contribution of the components at 1566 cm^{-1} in the deconvolution of HC (Fig. 2c), and at 1555 and 1538 cm^{-1} in the deconvolution of ConBr (Fig. 2d).

It is worth mentioning that the components at 1632, 1617 and 1550 cm^{-1} are located in the vibration interval of primary (NH_3^+) and secondary (NH_2^+) amine salts and also of C=O stretching of carboxyl ion (Fig. 2e) [35, 36]. Such attributions combined with the differences in line profile observed in the spectra of HC–ConBr, HC and ConBr indicate that lectin was immobilized on the support by electrostatic interaction.

Even though the immobilization of the ConBr on the HC occurred to some extent from electrostatic forces, other interactions could also account for the protein attachment and stabilization [46, 47]. The hydrochar used in this work was obtained after 24 h of reaction, and hydrothermal carbonization generates carbonaceous materials through cascade processes, for which the major one is dehydration [23–25, 27, 28, 48]. Therefore, reaction time influences the amount of oxygenated groups present on the surface of the HC, so that the longer the reaction time, the more oxygenated groups could be lost to the reaction medium. Such a fact could lead to the formation of more hydrophobic aromatic domains. It is also known that reaction time also influences HC particle size, promoting the formation of larger particles and aggregates at longer reaction times [27, 48, 49]. This means that larger particles have less oxygenated functional groups on their surface and more aromatic (hydrophobic) regions available [27].

In the case of the HC used in this work, a large reaction time could favor the formation of large particles with a non-homogenous distribution of oxygenated functional groups and, thus, with hydrophobic regions on the surface that might contribute to the interaction with the lectin. Then, it would be possible the interaction between these regions of the hydrothermal carbon and the central part of the tetrameric structure of the protein that is also hydrophobic. The occurrence of hydrophobic interactions in the HC–ConBr system is supported by the work of Perry and Puddu [46], who confirmed the manifestation of these interactions between neutral and negatively or positively charged peptides with different amino acid sequences and silica nanoparticles, which have negatively charged surfaces. Thus, other types of non-covalent interactions could be established in the lectin–HC interaction besides that of electrostatic attraction.

To demonstrate the immobilization of the protein on the hydrothermal carbon, an adsorption experiment using ConBr marked with FITC (ConBr–FITC) was performed. This sample was analyzed by confocal scanning laser microscopy. In Fig. 3a, it can be seen that ConBr–FITC has green fluorescence emission that can also be verified in HC–ConBr–FITC sample (Fig. 3b). Since pure HC or MES buffer does not have any type of fluorescent emission (Fig. S4) and the fluorescent marker is covalently bound to the lectin, the green color observed in the emission of the sample HC–ConBr–FITC indicates the presence of the immobilized protein on the surface of the hydrothermal carbon.

In order to evaluate the activity of the protein immobilized on the hydrothermal carbon, hemagglutination assays were performed. Light microscopy images presented in Fig. 4a, b show assays performed for ConBr (positive control) and HC (negative control), respectively. The controls of pure erythrocytes in Tris–HCl and MES buffer are shown in Fig. S5. In Fig. 4a, the formation of clots is seen, whose formation is a characteristic property of ConBr. In Fig. 4b, there is no sign of erythrocyte agglutination. What can be seen instead is the HC forming agglomerates among the erythrocytes, with no signs of coagulation. In Fig. 4c, it can be seen that HC–ConBr has the ability to agglutinate erythrocytes and the image shows different sized clots distributed over the slide. Dark points in the interior and edges of clots indicate the presence of HC and reinforce the hypothesis that the lectin is adsorbed onto the surface
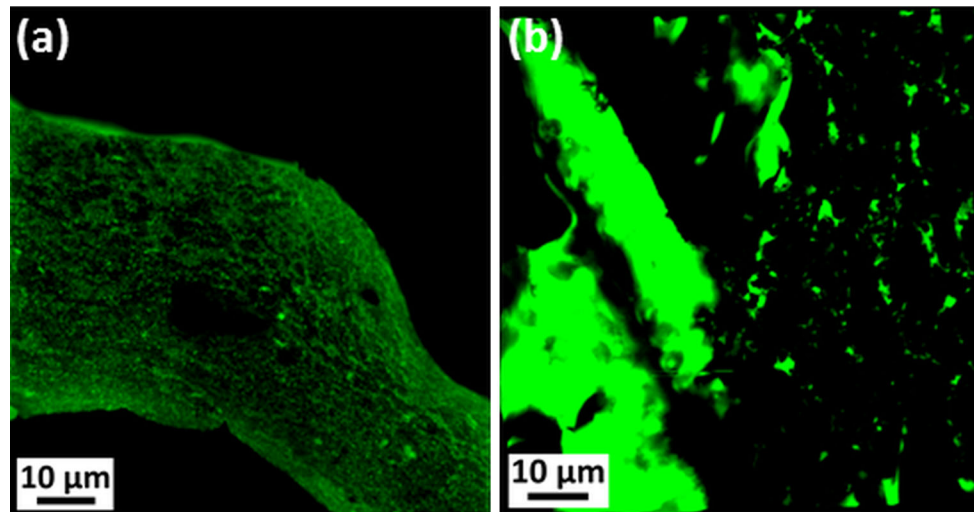
Figure 3 Fluorescence emission analysis by confocal scanning laser microscopy. **a** ConBr–FITC and **b** HC–ConBr–FITC.
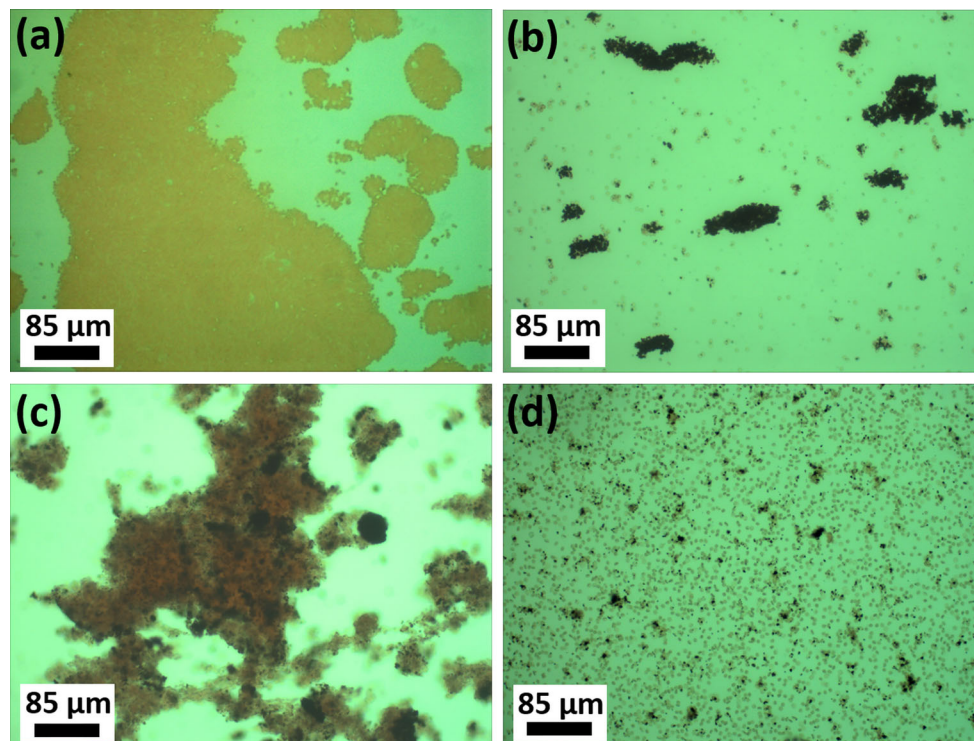

Figure 4 Evaluation of hemagglutination activity assays by light microscopy. **a** ConBr, **b** HC, **c** HC–ConBr and **d** inhibition of hemagglutination activity of HC–ConBr with methyl-α-D-mannopyranoside.

of the carbonaceous material, since pure HC does not interact with erythrocytes. The agglutination inhibition assay (Fig. 4d) confirms that the hemagglutination activity observed in HC–ConBr is due to the presence of the lectin. After exposure of the sample to methyl-α-D-mannopyranoside, it does not interact with erythrocytes due to a "blockage" of its CRD by the sugar, and hence, there is no formation of clots.

Conclusions

Results obtained in this work suggest that HC can be used as a support to immobilize biomolecules (e.g., ConBr lectin), in a manner that the protein preserves its properties. The analysis of primary and secondary amines and carboxylic acid groups in the FTIR spectra indicates that the interaction between HC and

ConBr occurs mainly via electrostatic interactions. However, the possibility of hydrophobic interactions could not be discarded. In addition, the ConBr hemagglutination activity (toward red blood cells) was preserved after its immobilization. Finally, the non-covalent method used here constitutes a simple, inexpensive and effective way of immobilizing proteins on HC.

Acknowledgements

Electronic supplementary material: The online version of this article (doi:10.1007/s10853-017-1441-7) contains supplementary material, which is available to authorized users.

References

[1] Sheldon RA, van Pelt S (2013) Enzyme immobilisation in biocatalysis: why, what and how. Chem Soc Rev 42:6223–6235. doi:10.1039/C3CS60075K

[2] Benešová E, Králová B (2012) Affinity interactions as a tool for protein immobilization. In: Magdeldin S (ed) Affinity chromatography. InTech, Rijeka, pp 29–46

[3] Calvaresi M, Zerbetto F (2013) The devil and holy water: protein and carbon nanotube hybrids. Acc Chem Res 46:2454–2463. doi:10.1021/ar300347d

[4] Singh S, Vardharajula S, Tiwari P et al (2012) Functionalized carbon nanotubes: biomedical applications. Int J Nanomedicine 7:5361–5374. doi:10.2147/IJN.S35832

[5] Elnashar MM (2010) Immobilized molecules using biomaterials and nanobiotechnology. J Biomater Nanobiotechnol 1:61–77. doi:10.4236/jbnb.2010.11008

[6] Bhakta SA, Evans E, Benavidez TE, Garcia CD (2015) Protein adsorption onto nanomaterials for the development of biosensors and analytical devices: a review. Anal Chim Acta 872:7–25. doi:10.1016/j.aca.2014.10.031

[7] Kaushik M, Sinha P, Jaiswal P et al (2016) Protein engineering and de novo designing of a biocatalyst. J Mol Recognit 29:499–503. doi:10.1002/jmr.2546

[8] Eş I, Vieira JDG, Amaral AC (2015) Principles, techniques, and applications of biocatalyst immobilization for industrial application. Appl Microbiol Biotechnol 99:2065–2082. doi:10.1007/s00253-015-6390-y

[9] Hernandez K, Fernandez-Lafuente R (2011) Control of protein immobilization: coupling immobilization and site-directed mutagenesis to improve biocatalyst or biosensor performance. Enzyme Microb Technol 48:107–122. doi:10.1016/j.enzmictec.2010.10.003

[10] Bilal M, Iqbal HMN, Hussain Shah SZ et al (2016) Horseradish peroxidase-assisted approach to decolorize and detoxify dye pollutants in a packed bed bioreactor. J Environ Manag 183:836–842. doi:10.1016/j.jenvman.2016.09.040

[11] Ensuncho L, Alvarez-Cuenca M, Legge RL (2005) Removal of aqueous phenol using immobilized enzymes in a bench scale and pilot scale three-phase fluidized bed reactor. Bioprocess Biosyst Eng 27:185–191. doi:10.1007/s00449-005-0400-x

[12] De Schutter K, Van Damme E (2015) Protein–carbohydrate interactions as part of plant defense and animal immunity. Molecules 20:9029–9053. doi:10.3390/molecules20059029

[13] De Vasconcelos MA, Cunha CO, Sousa Arruda FV et al (2012) Lectin from *Canavalia brasiliensis* seeds (ConBr) is a valuable biotechnological tool to stimulate the growth of *Rhizobium tropici* in vitro. Molecules 17:5244–5254. doi:10.3390/molecules17055244

[14] Cavada BS, Barbosa T, Arruda S et al (2001) Revisiting proteus: do minor changes in lectin structure matter in biological activity? Lessons from and potential biotechnological uses of the Diocleinae subtribe lectins. Curr Protein Pept Sci 2:123–135. doi:10.2174/1389203013381152

[15] Bento CAM, Cavada BS, Oliveira JTA et al (1993) Rat paw edema and leukocyte immigration induced by plant lectins. Agents Actions 38:48–54. doi:10.1007/BF02027213

[16] Barral-Netto M, Santos SB, Barral A et al (1992) Human lymphocyte stimulation by legume lectins from the diocleae tribe. Immunol Invest 21:297–303. doi:10.3109/08820139209069369

[17] Barauna S, Kaster M, Heckert B et al (2006) Antidepressant-like effect of lectin from *Canavalia brasiliensis* (ConBr) administered centrally in mice. Pharmacol Biochem Behav 85:160–169. doi:10.1016/j.pbb.2006.07.030

[18] Jacques AV, Rieger DK, Maestri M et al (2013) Lectin from *Canavalia brasiliensis* (ConBr) protects hippocampal slices against glutamate neurotoxicity in a manner dependent of PI3K/Akt pathway. Neurochem Int 62:836–842. doi:10.1016/j.neuint.2013.02.020

[19] Silva FO, Santos PN, Figueirôa EO et al (2014) Antiproliferative effect of *Canavalia brasiliensis* lectin on B16F10 cells. Res Vet Sci 96:276–282. doi:10.1016/j.rvsc.2014.01.005

[20] Nagaraju K, Reddy R, Reddy N (2015) A review on protein functionalized carbon nanotubes. J Appl Biomater Funct Mater 13:e301–e312. doi:10.5301/jabfm.5000231

[21] Yang Y, Asiri AM, Tang Z et al (2013) Graphene based materials for biomedical applications. Mater Today 16:365–373. doi:10.1016/j.mattod.2013.09.004

[22] Wang J, Qiu J (2016) A review of carbon dots in biological applications. J Mater Sci 51:4728–4738. doi:10.1007/s10853-016-9797-7

[23] Falco C, Perez Caballero F, Babonneau F et al (2011) Hydrothermal carbon from biomass: structural differences between hydrothermal and pyrolyzed carbons via 13 C solid state NMR. Langmuir 27:14460–14471. doi:10.1021/la202361p

[24] Yu L, Falco C, Weber J et al (2012) Carbohydrate-derived hydrothermal carbons: a thorough characterization study. Langmuir 28:12373–12383. doi:10.1021/la3024277

[25] Hu B, Wang K, Wu L et al (2010) Engineering carbon materials from the hydrothermal carbonization process of biomass. Adv Mater 22:813–828. doi:10.1002/adma.200902812

[26] Titirici M-M, White RJ, Falco C, Sevilla M (2012) Black perspectives for a green future: hydrothermal carbons for environment protection and energy storage. Energy Environ Sci 5:6796–6822. doi:10.1039/c2ee21166a

[27] Sevilla M, Fuertes AB (2009) Chemical and structural properties of carbonaceous products obtained by hydrothermal carbonization of saccharides. Chem A Eur J 15:4195–4203. doi:10.1002/chem.200802097

[28] Titirici M-M, Antonietti M, Baccile N (2008) Hydrothermal carbon from biomass: a comparison of the local structure from poly- to monosaccharides and pentoses/hexoses. Green Chem 10:1204–1212. doi:10.1039/b807009a

[29] Moreira RA, Cavada BS (1984) Lectin from *Canavalia brasiliensis* (MART.). Isolation, characterization and behavior during germination. Biol Plant 26:113–120

[30] Cavada BS, Santos CF, Grangeiro TB et al (1998) Purification and characterization of a lectin from seeds of *Vatairea macrocarpa* Duke. Phytochemistry 49:675–680. doi:10.1016/S0031-9422(98)00144-7

[31] Bradford MM (1976) A rapid and sensitive method for the quantitation of microgram quantities of protein utilizing the principle of protein-dye binding. Anal Biochem 72:248–254. doi:10.1016/0003-2697(76)90527-3

[32] Ainouz IL, Sampaio AH, Benevides NMB et al (1992) Agglutination of enzyme treated erythrocytes by Brazilian marine algal extracts. Bot Mar 35:475–479. doi:10.1515/botm.1992.35.6.475

[33] Wang H, Ma L, Cao K et al (2012) Selective solid-phase extraction of uranium by salicylideneimine-functionalized hydrothermal carbon. J Hazard Mater 229–230:321–330. doi:10.1016/j.jhazmat.2012.06.004

[34] Pavia DL, Lampman GM, Kriz GS (2001) Introduction to spectroscopy: a guide for students of organic chemistry, 3rd edn. Thomson Learning Inc, Stamford

[35] Patnaik P (2004) Dean's analytical chemistry book, 2nd edn. McGRAW-HILL, New York

[36] Silverstein RM, Webster FX, Kiemle DJ (2006) Identificação Espectrométrica de Compostos Orgânicos, 7th edn. LTC, Rio de Janeiro

[37] Geng W, Nakajima T, Takanashi H, Ohki A (2009) Analysis of carboxyl group in coal and coal aromaticity by Fourier transform infrared (FT-IR) spectrometry. Fuel 88:139–144. doi:10.1016/j.fuel.2008.07.027

[38] Nascimento KS, Rosa PAJ, Nascimento KS et al (2010) Partitioning and recovery of *Canavalia brasiliensis* lectin by aqueous two-phase systems using design of experiments methodology. Sep Purif Technol 75:48–54. doi:10.1016/j.seppur.2010.07.008

[39] Portal, ExPASy—Bioinformatics Resource (ProtParam Tool). http://web.expasy.org/cgi-bin/protparam/protparam1?P55915@1-237@. Accessed 8 Sep 2016

[40] Grangeiro TB, Schriefer A, Calvete JJ et al (1997) Molecular cloning and characterization of ConBr, the lectin of *Canavalia brasiliensis* seeds. Eur J Biochem 248:43–48. doi:10.1111/j.1432-1033.1997.00043.x

[41] Huet M, Claverie JM (1978) Sedimentation studies of the reversible dimer–tetramer transition kinetics of concanavalin A. Biochemistry 17:236–241. doi:10.1021/bi00595a007

[42] Barth A (2007) Infrared spectroscopy of proteins. Biochim Biophys Acta Bioenergy 1767:1073–1101. doi:10.1016/j.bbabio.2007.06.004

[43] Kong J, Yu S (2007) Fourier transform infrared spectroscopic analysis of protein secondary structures. Acta Biochim Biophys Sin (Shanghai) 39:549–559. doi:10.1111/j.1745-7270.2007.00320.x

[44] Nogueira KAB, Cecilia JA, Santos SO et al (2016) Adsorption behavior of bovine serum albumin on ZnAl and Mg–Al layered double hydroxides. J Sol-Gel Sci Technol 80:748–758. doi:10.1007/s10971-016-4166-1

[45] Alarcon EI, Bueno-Alejo CJ, Noel CW et al (2013) Human serum albumin as protecting agent of silver nanoparticles: role of the protein conformation and amine groups in the nanoparticle stabilization. J Nanoparticle Res. doi:10.1007/s11051-012-1374-7

[46] Puddu V, Perry CC (2012) Peptide adsorption on silica nanoparticles: evidence of hydrophobic interactions. ACS Nano 6:6356–6363. doi:10.1021/nn301866q

[47] Mu Q, Jiang G, Chen L et al (2014) Chemical basis of interactions between engineered nanoparticles and biological systems. Chem Rev 114:7740–7781. doi:10.1021/cr400295a

[48] Li R, Wang L, Shahbazi A (2015) A review of hydrothermal carbonization of carbohydrates for carbon spheres preparation. Trends Renew Energy 1:43–56. doi:10.17737/tre.2015.1.1.009

[49] Qi Y, Zhang M, Qi L, Qi Y (2016) Mechanism for the formation and growth of carbonaceous spheres from sucrose by hydrothermal carbonization. RSC Adv 6:20814–20823. doi:10.1039/C5RA26725K